

# Geological Appraisal and Mineralogical Characteristics of Iron Ore Occurrences around Neem Ka Thana Area in Khetri Basin, North Delhi Fold Belt, Rajasthan, Western India

Sigma Dwivedy

P.G. Department of Geology, Utkal University, Bhubaneswar-4, Odisha, India

Corresponding Author Email: [zigmastigma\[at\]gmail.com](mailto:zigmastigma[at]gmail.com)

**Abstract:** *Lensoidal iron ore bodies occur within the meta sediments of Ajabgarh Group of rocks in North Delhi Fold Belt and are exposed around Neem Ka Thana area of Rajasthan. The moderate to steeply dipping iron ore bodies continue from 100 m to 1.5 km along the strike direction with the variable width from 2 m to 5 m. The ore bodies occur within the metapelite rocks comprising of micaceous phyllite, albitised phyllite and feldspathic quartzite. In some cases, albitite, pegmatite and quartz carbonate veins are seen to be intruded into the iron ore bodies. Detailed petrographic studies of the iron ore sample suggest a dominant hematite, magnetite and specularite composition with minor goethite cores. Based on the geological disposition, ore mineral assemblages, textural characteristics and host rock association, the iron ores in the areas are thought to be deposited by hydrothermal IOCG type deposits.*

**Keywords:** Iron-Oxide-Copper-Gold (IOCG), Hydrothermal magnetite, Soda-metasomatism, Albitite

## 1. Introduction

The Iron oxides (magnetite and hematite) are very common minerals in both magmatic and metamorphic rocks. These are also found as major to accessory minerals in other mineral deposits. Even though iron ore mineralization is enormously found in banded iron formation but these are also very much productive in Iron-Oxide-Copper-Gold (IOCG), Kiruna-type apatite-magnetite, porphyry systems iron skarn and magmatic Fe-Ti deposits. Iron ores found in study area are mainly located in the eastern and south-eastern part of Khetri basin (surrounding Neem Ka Thana area). The areas belong to Alwar and Ajabgarh Groups of Delhi Supergroup having NE-SW trending axial traces. The moderate to steeply dipping iron ore bodies continue from 100 m to 1.5 km along the strike direction with variable width from 2 m to 5m. The major ore minerals are hematite and magnetite along with some specularite. The ore bodies occur within the metapelitic rocks comprising of micaceous phyllite, albitised phyllite and feldspathic quartzite etc. Here we describe the petrographic study, XRD, EPMA analyses of the iron ores at Neem Ka Thana, with a broad understanding with its genesis and evolution.

## 2. Geological settings

The rocks of Proterozoic fold belts of Aravalli-Delhi province are specifically characterized by the older Aravalli

Supergroup and the younger Delhi Supergroup. The southern and south-eastern part of Rajasthan is mainly occupied by Aravalli Supergroup while the south-western and north-eastern part occupied by Delhi Supergroup. Aravalli Supergroup is constituted by a wide sequence of clastic sediments with interbedded basic volcanic rocks with a complex deformations and diverse depositional environments. The Aravalli Supergroup rests unconformably over the oldest basement (~3.3-2.5 Ga) Banded gneissic complex (BGC). The major constituent is mainly of granites, pegmatites, and granitic gneisses with minor meta-volcano sedimentary rocks (Heron, 1953; Gopalan et al., 1990; Golani et al., 2002). The older Palaeo-Proterozoic Aravalli Fold Belt (2.2–1.85 Ga) and younger Mesoproterozoic Delhi Fold Belt (1.8–0.85 Ga) lie over the basement BGC complex collectively known as the Aravalli-Delhi fold belt (ADFB) (Fig.1) (Roy, 1988; Kaur et al., 2011). The NDFB comprises three subparallel rift basins named as Lalsot-Bayana, Alwar, and Khetri basins (Sinha-Roy et al., 2013). In western part of the Delhi fold belt (DFB), Khetri basin is situated where the study areas lie. The basement volcano-metamorphic complex (BGC), overlain by the psammite of Alwar and the pelite of Ajabgarh Group with different granitic intrusions constitutes the Khetri basin (Fig.1).

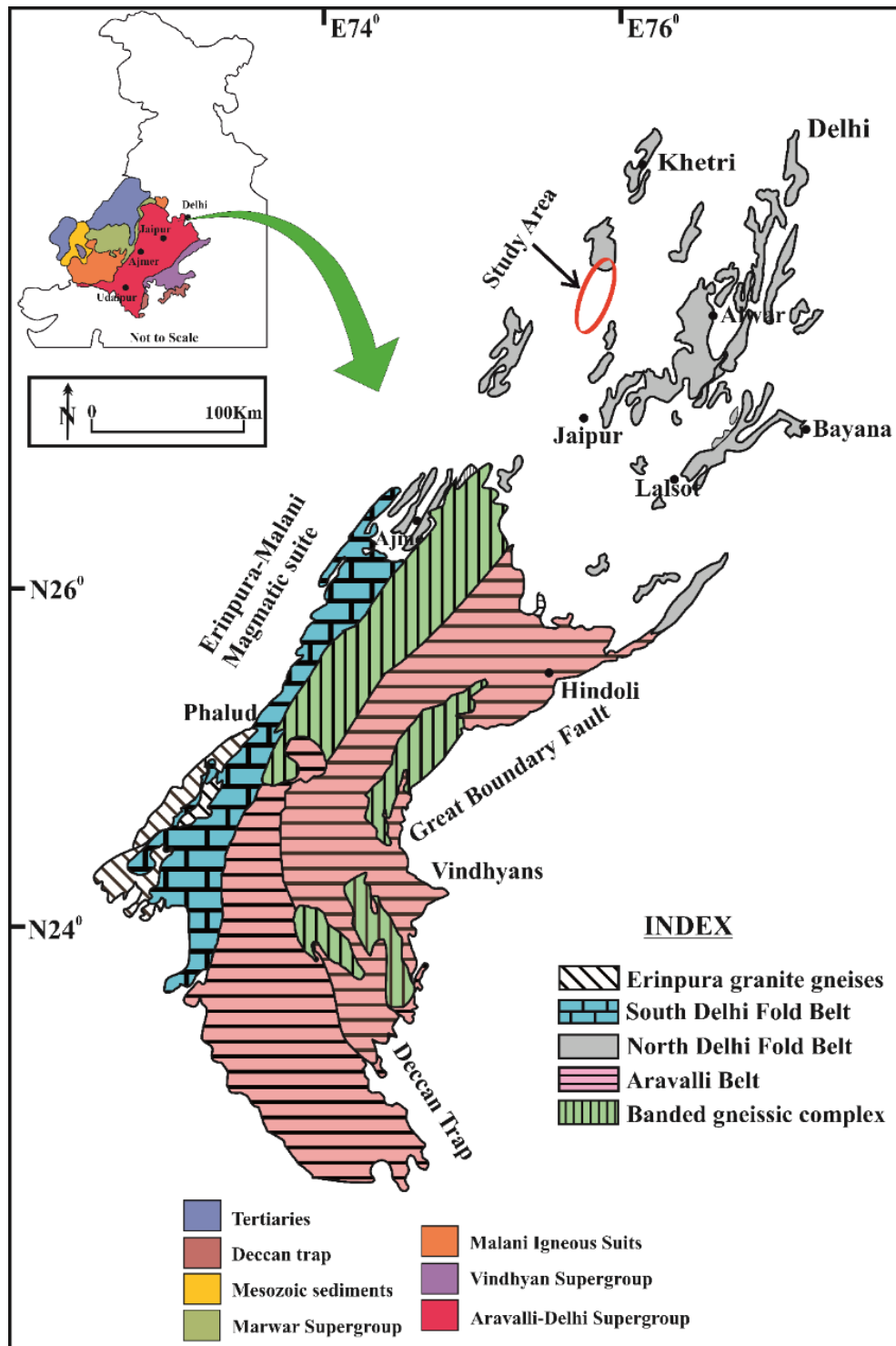


**Figure 1:** Simplified geological map of the Aravalli-Delhi Fold Belt showing the study area (after Roy, 1988) showing the study area (marked within the red ellipse)

### 3. Methodology

Fresh iron ore and its associated host rock samples were collected from the quarries of iron ore located around the Neem-Ka-Thana area. The samples are examined under reflected and transmitted light microscope. Detailed petrography of the samples helped to understand the mineralogical characteristics, textural properties and the nature of mineralization. The XRD and EPMA studies was carried out to better understand the mineral phases present and quantify the elemental concentration present in minerals. A total of 20 thin polished sections collected from Nanagwas,

Raipur, and, Jaitpura representing the eastern flank, and Bagholi and Karath representing the western flank were studied for comparison of the mineralization and effects of Na-metasomatism. The major and some trace elements of magnetite are analysed by CAMECA (SX-5) Electron Probe Micro Analyzer at Central Research Facilities in Indian Institute of Technology (Indian School of Mines), Dhanbad, India. The analysis has been carried out for Na, Al, Fe, Si, F, Mg, Ca, Ti, Mn, P, K and Cr using the mode of wavelength dispersion with a beam current of 15nA, excitation voltage of 15 kV with a beam size of 1  $\mu$ m.

#### 4. Field Overview

Iron-ore mineralization is located in the district of Jhunjhunu and Sikar in the toposheets no.45M/9,10,13,14 within the state of Rajasthan, north-western India. The mineralized areas are situated around the Neem-Ka-Thana area which is located in the southern or southeastern part of the Khetri Copper Belt (Fig 1). The hills present in this area follow the linear trend of the NNE-SSW direction. Iron ores are mineralized along the hill flank of this area. The field observation suggests that there are numerous steeply dipping pocket type medium to

high grade (44.10% to 65% Fe) iron ore bodies are associated with albitite and metasedimentary rocks (Fig. 2 A, B). The host rocks are mainly comprised of micaceous phyllite, albitised phyllite, and feldspathic quartzite, and in some cases, albitite, pegmatite, and quartz-carbonate-fluorite veins are intruded into the iron ore bodies (Fig. 2 C). The intruded veinlets of magnetite into the albitite rocks are also observed in some areas (Fig. 2D). Mineralogically, the iron ores are dominated by magnetite and hematite devoid of any sulfide phases which occur as massive, granular, and vein fillings within the host rocks (Dwivedy and Sahoo, 2021; Dwivedy, 2024).

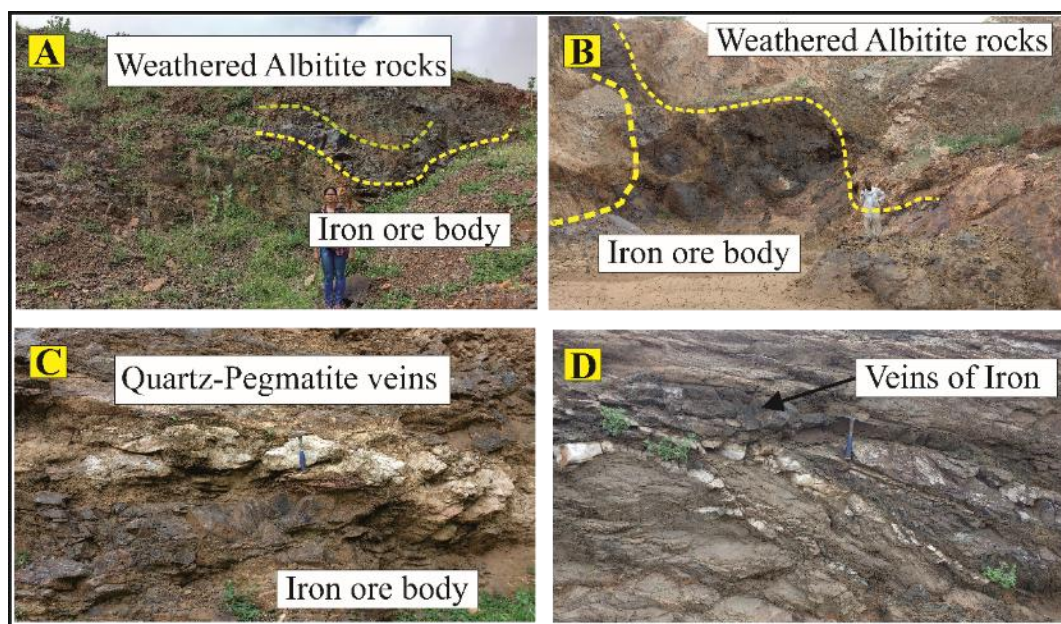


**Figure 2:** Field photographs showing (A)(B) Iron ore occurrences in weathered albitite rocks ;(C) Quartz-pegmatite veins with the remnant of iron ore ;(D) Occurrence of magnetite veins intruded into the albitite rock

#### 5. Petrographic Analysis and EPMA Studies

The iron ore found from the study areas is mainly comprised of oxide minerals such as massive magnetite, hematite, specularite (micaceous variety of hematite) in the form of vein filling that is devoid of any sulfide phases. Based on the ore petrography, magnetite has been identified as the dominant iron ore mineral followed by hematite and goethite in all the study areas (Fig.3). Most of the iron ores in the area consist of magnetite, which may have been partially altered into hematite along cracks, and the grain boundaries of the magnetite exhibit signs of oxidizing environments during mineralization process (Fig 3 A, B). Based on petrography studies, the nature of iron ore in the study area are mainly of massive and specular variety comprising of magnetite and hematite along with specularite. The massive ores are compact and densely packed with magnetite and hematite exhibiting magnetitisation and goethitisation process respectively (Fig. 3). Occasional botryoidal goethites have been observed along the boundary of magnetite grains also

demonstrate the oxidizing conditions that prevailed at the time of its mineralization. (Fig 3 C). The samples that are magnetitized, indicate the earlier relict magnetite phase in the deposit and suggestive of oxidation due to hydrothermal fluids. In some of the areas iron ores are micaceous in variety called as specularite, (Fig. 3D) show the hematite grains are lath shaped elongated in nature. The grains of specularite are disseminated and randomly within quartz, biotite, muscovite, phlogopite, fluoro apatite, fluorite and minor monazite etc (Fig. 3E). The phlogopite, apatite, occurrence of fluorite veins, xenotime/monazite signifies the hydrothermal emplacement along the ore formation. EPMA studies conducted on the ore and host rocks assemblages confirm the presence of altered magnetite, hematite, and rare goethite as the iron-bearing ore minerals (Table 1). Apart from the magnetite, hematite, and goethite, feldspar (Albite, Oligoclase, Orthoclase), phlogopite biotite, muscovite, amphibole (actinolite), and accessory minerals like apatite, monazite, ilmenite, and sphene were detected during the EPMA studies (Table -2) (Fig 3 E, F).

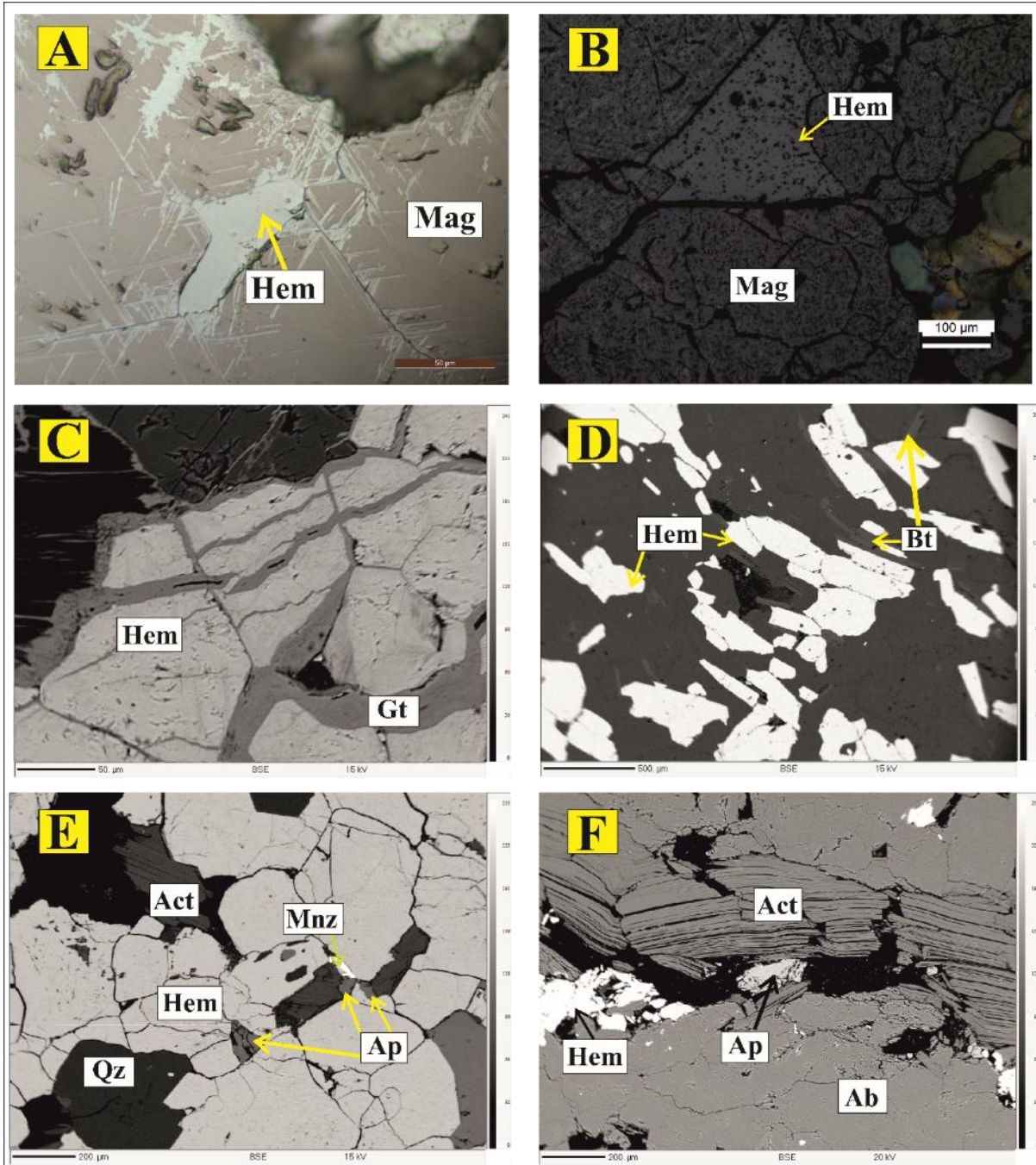


**Figure 3:** Field photographs and BSE images showing (A)(B) Hematite replacement along the octahedral cleavage planes of magnetite as recorded in the massive ores of from Raipur; (C) Formation of goethite at around the grain boundary of magnetite grains ;(D) Specular hematite grain occurrence within the phyllitic rocks;(E) Occurrences of monazite grain within hematite grains and closely associated with the apatite;(F) Presence of fluorapatite in association with the hematite assemblage in the Actinolite and albitites.

**Table 1:** EPMA studies of iron ores in the study area.

SiO <sub>2</sub>	Al <sub>2</sub> O <sub>3</sub>	FeO	TiO <sub>2</sub>	MgO	CaO	MnO	Cr <sub>2</sub> O <sub>3</sub>	Na <sub>2</sub> O	K <sub>2</sub> O	P <sub>2</sub> O <sub>5</sub>	Total	Mineral
0.03	0.11	<b>91.31</b>	nd	<b>0.06</b>	0.04	0.07	nd	0.03	nd	nd	91.65	<b>Magnetite</b>
0.03	0.03	<b>91.93</b>	0.09	<b>0.05</b>	nd	0.08	0.02	nd	0.02	nd	92.25	<b>Magnetite</b>
0.01	0.09	<b>92.15</b>	0.05	<b>0.01</b>	nd	0.01	0.05	0.02	0.02	nd	92.41	<b>Magnetite</b>
0.05	0.05	<b>88.58</b>	0.17	<b>0.05</b>	0.02	0.1	0.04	0.04	0.06	0.02	89.18	<b>Hematite</b>
nd	0.04	<b>87.38</b>	0.67	<b>0.01</b>	0.02	nd	0.01	0.05	0.02	nd	88.2	<b>Hematite</b>
0.02	0.01	<b>86.52</b>	0.06	<b>0.01</b>	nd	0.04	nd	nd	nd	0.07	86.73	<b>Hematite</b>
0.02	nd	<b>86.26</b>	0.06	<b>nd</b>	0.02	0.03	nd	nd	0.01	0.05	86.45	<b>Hematite</b>
4.23	0.77	<b>70.25</b>	nd	<b>0.1</b>	0.1	0.1	0.03	0.02	nd	0.11	75.71	<b>Goethite</b>
4.55	1.91	<b>69.01</b>	0.01	<b>0.08</b>	0.14	0.05	nd	0.04	nd	0.19	75.98	<b>Goethite</b>
2.68	1.05	<b>76.52</b>	0.04	<b>0.07</b>	0.21	nd	nd	0.11	0.02	1.36	82.06	<b>Goethite</b>
0.15	0.06	<b>86.36</b>	0.01	<b>0.02</b>	0.05	0.03	0.01	nd	nd	0.04	86.73	<b>Hematite</b>
4.54	1.61	<b>68.79</b>	0.04	<b>0.05</b>	0.13	0.09	nd	0.07	0.01	0.13	75.46	<b>Goethite</b>

0.05	0.79	<b>88.76</b>	0.87	nd	nd	0.07	0.01	nd	nd	nd	90.55	<b>Hematite</b>
nd	0.78	<b>89.95</b>	0.89	nd	0.01	0.04	0.01	0.02	0.01	nd	91.71	<b>Magnetite</b>
0.02	0.79	<b>88.21</b>	0.83	<b>0.04</b>	0.05	0.03	0.03	0.02	nd	0.05	90.07	<b>Hematite</b>
0.01	0.71	<b>87.36</b>	1.06	nd	nd	nd	0.01	0.02	nd	nd	89.17	<b>Hematite</b>
0.03	0.66	<b>87.6</b>	1.07	nd	0.01	0.08	nd	nd	0.01	nd	89.46	<b>Hematite</b>
0.02	0.72	<b>88.23</b>	1.12	<b>0.01</b>	0.02	nd	0.02	0.03	0.02	0.01	90.2	<b>Hematite</b>

**Table-2:** EPMA results of minerals associated with iron ores in the study area.

SiO <sub>2</sub>	Al <sub>2</sub> O <sub>3</sub>	FeO	TiO <sub>2</sub>	MgO	CaO	MnO	Cr <sub>2</sub> O <sub>3</sub>	Na <sub>2</sub> O	K <sub>2</sub> O	P <sub>2</sub> O <sub>5</sub>	F	Total	Mineral
0.02	nd	45.01	50.96	0.43	0.01	3.73	nd	0.03	nd	nd	nd	100.13	Ilmenite
0.02	nd	46.58	45.9	0.32	0.03	3.71	0.02	nd	nd	0.01	nd	96.58	Ilmenite
29.16	0.58	1.11	38.71	0.01	28.15	nd	0.02	0.04	0.03	0.09	0.12	98.02	Sphene
29.01	0.52	0.89	38.45	nd	27.33	0.06	0.04	0.02	nd	0.07	0.06	96.45	Sphene
62.77	15.57	0.12	nd	0.01	0.03	0.01	0.02	0.27	16.11	0.01	0.01	94.93	Orthoclase
62.46	15.84	0.92	0.05	0.01	nd	0.03	nd	0.54	15.7	nd	0.1	95.65	Orthoclase
68.73	17.54	0.2	0.03	0.23	0.28	0.02	nd	10.34	0.08	nd	nd	97.45	Albite
69.25	17.7	0.01	0.04	nd	0.07	nd	0.03	10.61	0.03	0.01	nd	97.68	Albite
0.2	nd	0.04	0.03	nd	54.79	0.06	nd	0.15	nd	42.26	3.16	100.69	Apatite
0.29	nd	0.21	0.01	nd	53.83	0.14	nd	0.17	0.01	41.49	3.1	99.25	Apatite
97.91	nd	0.22	0.02	nd	0.04	nd	0.01	nd	0.01	0.01	nd	98.22	Quartz
98.11	nd	0.11	0.03	nd	0.02	0.06	nd	0.02	nd	0.02	0.01	98.38	Quartz
51.74	1.72	12.15	0.22	15.21	11.97	0.07	0.06	0.66	0.37	nd	0.32	94.48	Actinolite

### 6. Result and Discussion

From the mineral chemistry (EPMA) of magnetite, FeO ranges from 69.01-92.15 wt.%, Al<sub>2</sub>O<sub>3</sub> 0.01 – 1.61 wt.%, TiO<sub>2</sub> 0.01–1.12 wt.%, MnO 0.01–0.1 wt.%, Cr<sub>2</sub>O<sub>3</sub> 0.01-0.1wt.% and V% 0.01–0.09 wt.% are present as minor oxides. Detailed ore petrography, textural patterns, lithological assemblages, age of mineralization and mineral chemistry of the iron ore suggest a magmatic source precipitated by hydrothermal process. From the field overview the iron ore is mainly hosted in mainly metapelitic/meta marl and albitized quartzitic rocks. All these rocks were governed by multiple deformation and poly metamorphism and hydrothermal alteration might have taken the primary role in elemental distribution patterns in this iron mineralization. At some occurrences, criss-cross veins of quartz, calcite, fluorite, pegmatite, and albitite are found within these iron bodies, is suggesting evidence of

multiple episodes of hydrothermal/metasomatic activities. From the petrographic and EPMA analysis, it is confirmed that some grains of fluorapatite is associated with both the iron ores and the host rocks, which may support the involvement of hydrothermal activity in the study area. The comparison in between Ti and V concentrations can differentiate the igneous magnetite from hydrothermal magnetite. The concentration of Al, Ti, V is generally higher in igneous magnetite than hydrothermal magnetite. The concentration of V in typical hydrothermal magnetite shows a lower value <1000 ppm (Rusk et al., 2009). The ratio of V/Ti from the magnetite in study areas is showing a value >1, which further supports the hydrothermal origin. By the use of Ni/(Cr+Mn) vs. Ti+V (Fig. 4A), the Ca+Al+Mn vs. Ti+V (Fig. 4B) and Al+Mn vs. Ti+V (Fig.4 C) discriminant diagrams, most of the magnetite grains from the study area plot in the field of IOCG setup.

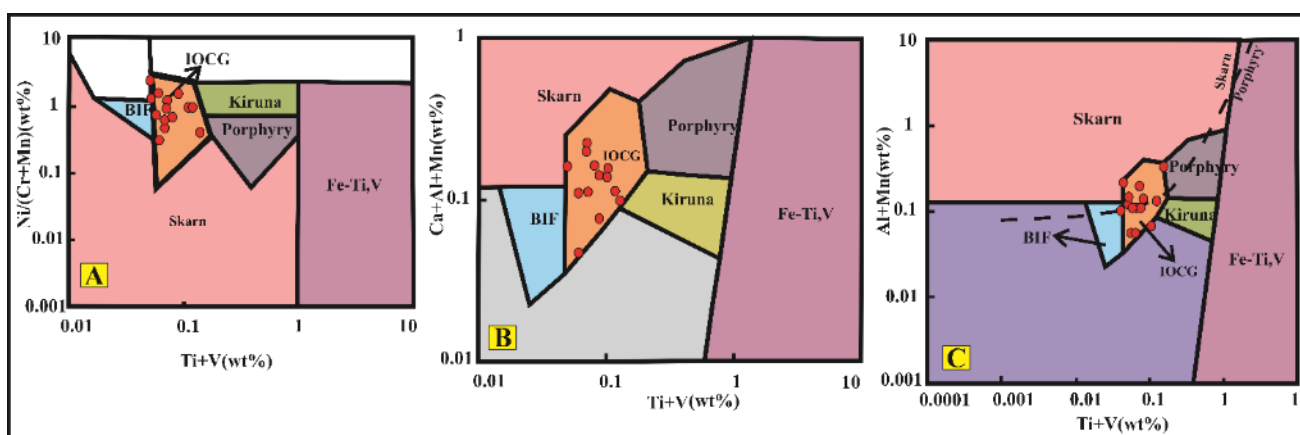


**Figure 4:** (A) Ni/(Cr+Mn) vs. Ti+V ;(B) Ca+Al+Mn vs. Ti+V; (C) Al+Mn vs. Ti+V, suggesting IOCG deposits model based on magnetite EPMA data (Dupuis and Beaudoin, 2011).

### 7. Conclusion

Iron ores from the study areas has a variable and distinct concentrations of Ti, Al, Mg, Mn, V, Cr, Co, Ni and P. Iron-oxide mineralization hosted mainly in albitites, metapelites, quartzites and meta-sediments of the Paleoproterozoic age.

The crisscross pattern of albitite veins in iron ore bodies and vice versa suggests a multiple events of soda-metasomatism/hydrothermal activity in the area which is a plausible cause for the precipitation of iron ore. Development of albitites along with calcites, martite and titanite also represent the evidences of multiple phases of alteration

processes in this area. Detailed petrography and EPMA of magnetite provided important clues regarding the genetic environment in which iron has formed. This study suggests that the magnetite mineralization is evidence of hydrothermal IOCG setup.

is working as a contractual Assistant Professor at Utkal University, Bhubaneswar, Odisha, India.

## References

- [1] Beaudoin G., Dupuis C., Gosselin P., Jébrak M., 2007. Mineral chemistry of iron oxides: application to mineral exploration In: Andrew CJ (ed) Ninth Biennial SGA Meeting. Society for geology Applied to Mineral Deposits, Dublin, pp 497-500.
- [2] Dupuis, C., Beaudoin, G., 2011. Discriminant diagrams for iron oxide trace element fingerprinting of mineral deposit types. *Mineral. Deposita* 46, 319–335
- [3] Dwivedy, S., Sahoo, P.R., 2021. Geology and trace element geochemistry of the albitite hosted iron ore mineralization around Khetri copper deposit, India: implications for an IOA type deposit. *Ore Geol. Rev.* 138, 104343.
- [4] Dwivedy. S., 2024. Petrogenetic implications, geochemistry and tectonic framework of albitite hosted magnetite in North Delhi Fold Belt: Application of geochemistry and apatite chemistry. *Geochemistry* 84,126176.
- [5] Golani, P.R., Pandit, M.K., Sial, A., Fallick, A.E., Ferreira, V.P., Roy, A.B., 2002. B-Na rich Paleoproterozoic Aravalli metasediments of evaporitic association, NW India: a new repository of gold mineralization. *Precamb. Res.* 116, 183–198.
- [6] Gopalan, K., Macdougall, J.D., Roy, A.B., Murli, A.V., 1990. Sm–Nd evidence for 3.3 Ga old rocks in Rajasthan, north western India. *Precamb. Res.* 48, 287-297.
- [7] Heron, A.M., 1953. The geology of central Rajputana. *Memoirs of the Geological Survey of India.* 79, 389.
- [8] Kaur, P., Chaudhri, N., Raczek, I., Kröner, A., Hofmann, A.W., Okrusch, M., 2011. Zircon ages of late Palaeoproterozoic (ca. 1.72–1.70 Ga) extension-related granitoids in NE Rajasthan, India: regional and tectonic significance. *Gondwana Res.* 19, 1040–1053.
- [9] Roy, A.B., 1988. Stratigraphic and tectonic framework of the Aravalli Mountain Range. In *Precambrian of the Aravalli Mountain, Rajasthan, India*, A.B.Roy (Ed.). *Mem. Geological society of India*, 7, 3-31.
- [10] Rusk, B.G., Oliver, N., Brown, A., Lilly, R., Jungmann, D., 2009. Barren magnetite breccias in the Cloncurry region, Australia; comparisons to IOCG deposits. In: Williams, P. J. (Ed.), *Proceedings of the 10th Biennial SGA Meeting of the Society for Geology Applied to Mineral Deposits*. The Society for Geology Applied to Mineral Deposits, Townsville Australia, 656–658.
- [11] Sinha-Roy, S., Malhotra, G., Mohanty, M., 2013. *Geology of Rajasthan*, Geological Society of India, Bangalore.

## Author Profile



**Dr. Sigma Dwivedy** received the PhD degree in geochemistry from IIT(ISM) Dhanbad, Jharkhand, India and M.Sc. and B.Sc. degrees in Geology from Ravenshaw University, Cuttack, Odisha, India. Now she